Imbalanced K^+ and Ca^{2+} subthreshold interactions contribute to increased hypothalamic presympathetic neuronal excitability in hypertensive rats

P. M. Sonner[1], S. Lee[2], P. D. Ryu[2], S. Y. Lee[2] and J. E. Stern[1]

[1] *Department of Physiology, Medical College of Georgia, Augusta, GA, USA*
[2] *Laboratory of Veterinary Pharmacology, Seoul National University, Seoul, South Korea*

Non-technical summary Despite the importance of brain-mediated sympathetic activation in the morbidity and mortality of patients with high blood pressure, the precise cellular mechanisms involved remain largely unknown. We show that an imbalanced interaction between two opposing currents mediated by potassium (I_A) and calcium (I_T) channels occurs in sympathetic-related hypothalamic neurons in hypertensive rats. We show that this imbalance contributes to enhanced membrane excitability and firing activity in this neuronal population. Knowledge of how these opposing ion channels interact in normal and disease states increases our understanding of underlying brain mechanisms contributing to the high blood pressure condition.

Abstract We investigated here whether an opposing interplay between the subthreshold currents A-type potassium (I_A) and T-type calcium (I_T) influences membrane excitability in presympathetic neurones of the hypothalamic paraventricular nucleus (PVN) that innervate the rostral ventrolateral medulla (RVLM). Moreover, we assessed whether a shift in the balance between these two subthreshold currents contributed to increased neuronal activity in hypertension. To this end, we obtained simultaneous electrophysiological recordings, confocal Ca^{2+} imaging, and single-cell RT-PCR samples from identified PVN-RVLM neurones in sham and renovascular hypertensive rats. Our results indicate that I_A and I_T, displaying overlapping voltage-dependent and kinetic properties, are present in PVN-RVLM neurones. We found that the relative predominance of each current at hyperpolarized membrane potentials dictates whether PVN-RVLN neurones express a low-threshold spike (LTS) or a transient outward rectification (TOR). Moreover, we report the I_A/I_T balance to be correlated with the relative expression of Kv4.3 and Cav3.1 subunit mRNA within individual neurones. Pharmacological blockade of I_A resulted in an enhanced I_T-mediated LTS, as well as LTS-mediated somatodendritic Ca^{2+} transients. In hypertensive rats, we found a shift in the I_T/I_A balance, towards an I_T predominance, due in part to a diminished Kv4.3 and enhanced Cav3.1 mRNA subunits expression. The imbalanced I_T/I_A relationship resulted in enhanced LTS, LTS-mediated somatodendritic Ca^{2+} transients, and increased firing activity in hypertensive rats. Taken together, our results support that a balanced I_T/I_A interaction influences membrane excitability and Ca^{2+} dynamics in PVN-RVLM neurones. Moreover, an imbalanced relationship favouring I_T results in enhanced neuronal excitability and firing discharge in hypertensive rats, constituting thus a likely mechanism contributing to the characteristic sympathoexcitation observed in this disease.

(Received 25 August 2010; accepted after revision 9 December 2010; first published online 13 December 2010)
Corresponding author Javier E. Stern: Department of Physiology, 1120 15th Street, Augusta, GA 30912, USA. Email: jstern@mcg.edu

Abbreviations 4-AP, 4 aminopyridine; I_A, A-type potassium current; I_T, T-type calcium current; LTS, low-threshold spike; OT, oxytocin; PVN, paraventricular nucleus; RVLM, rostral ventrolateral medulla; TEA, tetraethylammonium; TOR, transient outward rectification; VP, vasopressin.

DOI: 10.1113/jphysiol.2010.198556

Introduction

Neuronal excitability and firing activity within central neuronal circuits are tightly controlled by a fine-tuned balance between intrinsic membrane properties and synaptic inputs. Based on their voltage-dependent and kinetic properties, subthreshold currents such as the A-type potassium current (I_A) and the T-type calcium current (I_T) play a pivotal role in the control of membrane excitability within a critical range of membrane potentials near the threshold, influencing thus the frequency and pattern of Na^+-dependent action potentials fired by neurones.

I_A is a rapidly activating and inactivating transient outward current. Activation of I_A transiently decreases membrane excitability, delaying the onset of firing activity, restricting the duration of the action potential waveform, and increasing the interspike interval (Segal *et al.* 1984; Rogawski, 1985; Rudy, 1988; Fisher *et al.* 1998). Conversely, I_T is a transient inward current that when activated results in an increased neuronal excitability. A low-threshold spike (LTS) and burst firing discharge have been attributed to I_T (Llinas & Yarom, 1981; Tasker & Dudek, 1991; Stern, 2001). In addition, I_T has also been shown to regulate continuous firing activity (Raman & Bean, 1999), and the repolarization phase of the action potential waveform (McCobb & Beam, 1991; Lambert *et al.* 1998; Monteil *et al.* 2000).

Based on their overlapping voltage- and time-dependent properties, an opposing interplay between I_A and I_T has been shown to be critical in the control of neuronal excitability (Pape *et al.* 1994; Meis *et al.* 1996; Cavelier *et al.* 2003; Li *et al.* 2005; Molineux *et al.* 2005). Moreover, an altered balance in the I_T/I_A interaction was reported to contribute to hyperexcitability in pathological conditions, such as epilepsy (Meis *et al.* 1996).

The hypothalamic paraventricular nucleus (PVN) is a pivotal autonomic and neuroendocrine integrative centre, which plays a major role in the control of sympathetic outflow to the cardiovascular system (Swanson & Sawchenko, 1983; Coote *et al.* 1998; Dampney *et al.* 2005; Guyenet, 2006). These actions are mediated by presympathetic neurones that send direct projections to preganglionic neurones in the intermediolateral column of the spinal cord (Swanson & Kuypers, 1980; Lovick & Coote, 1988; Hosoya *et al.* 1991; Ranson *et al.* 1998), as well as to the rostral ventrolateral medulla (RVLM) (Ciriello *et al.* 1985; Dampney *et al.* 1987; Coote *et al.* 1998; Yang & Coote, 1998; Tagawa & Dampney, 1999; Kubo *et al.* 2000; Hardy, 2001; Allen, 2002). Accumulating evidence supports enhanced PVN neuronal activity as a key contributor to enhanced sympathetic outflow during pathological conditions, including hypertension, heart failure and diabetes (Patel, 2000; Allen, 2002; Zhu *et al.* 2004; Li & Pan, 2006; Zheng *et al.* 2006). Despite the impact of sympathoexcitation in the morbidity and mortality of these prevalent disorders (Esler & Kaye, 1998; Nesto, 2004), the precise underlying cellular mechanisms contributing to elevated PVN neuronal activity remain unknown.

Recently, we showed that I_A is a key factor regulating neuronal excitability in PVN-RVLM neurones (Sonner & Stern, 2007), and similarly to previous reports in other parvocellular PVN neurones (Luther & Tasker, 2000; Stern, 2001), we demonstrated the presence of I_T within this presympathetic neuronal population (Lee *et al.* 2007; Sonner *et al.* 2007; Lee *et al.* 2008). However, whether the interplay between I_A and I_T influences PVN-RVLM activity, and whether a shift in the balance between the two subthreshold currents contributes to increased excitability in disease conditions is at present unknown. We therefore, investigated in this study (a) whether there is an active interplay between I_A and I_T in PVN-RVLM neurones, (b) whether this interplay affects membrane properties and intracellular Ca^{2+} dynamics, and (c) whether a shift in the balance between these two conductances contributes to enhanced PVN neuronal activity during hypertension. To this end, we obtained simultaneous electrophysiological recordings, confocal Ca^{2+} imaging and single-cell RT-PCR samples from identified PVN-RVLM neurones in control rats, as well as in a well-established renovascular hypertensive animal model, in which a major contributing role for the PVN has been demonstrated (Earle *et al.* 1992; Earle & Pittman, 1995; Jung *et al.* 2004).

Methods

Ethical approval

Male Wistar rats ($n = 69$, 120–140 g) were purchased from Harlan laboratories (Indianapolis, IN, USA), and housed in a 12 h–12 h light–dark cycle with access to food and water *ad libitum*. All procedures were carried out in agreement with the Medical College of Georgia Animal Care and Use Committee's guidelines, and in compliance with NIH guidelines. Our experiments also comply with the policies and regulations of *The Journal of Physiology* (Drummond, 2009).

Renovascular surgery

Rats weighing between 150 and 180 g (approximately 5–6 weeks old) were used to induce the renovascular 2K1C Goldblatt hypertension model, a well characterized and widely used model (Martinez-Maldonado, 1991; Bergamaschi *et al.* 1995). As previously reported (Sonner *et al.* 2008), rats weighing between 150–180 g were maintained under anesthesia with isoflurane (3%).

Following an abdominal incision, the left kidney was exposed, and a 0.2 mm clip was placed over the left renal artery, partially occluding it (Carvalho *et al.* 2003). The sham procedure was the same, except the artery was not occluded. Post-operative care included proper management of associated pain (buprenorphine, 0.25 mg kg^{-1}, subcutaneous, as needed). All rats were used for experiments during the sixth to seventh week post-surgery. Blood pressure was measured at the beginning of the sixth week post-surgery, using a tail-cuff method. Values obtained were 137.9 ± 2.3 mmHg and 208.4 ± 3.1 mmHg in sham and hypertensive rats, respectively ($P < 0.0001$).

Retrograde labelling of PVN-RVLM neurones

Preautonomic RVLM-projecting PVN neurones were identified by injecting rhodamine beads unilaterally into the brainstem region containing the RVLM as previously described (Stern, 2001; Li *et al.* 2003). Rats were anaesthetized (ketamine–xylazine mixture, 90 and 50 mg kg^{-1}, respectively, I.P.) and a stereotaxic apparatus was used to pressure inject 200 nl of rhodamine-labelled microspheres (Lumaflor, Naples, FL, USA) into the RVLM (starting from Bregma: 12 mm caudal along the lamina, 2 mm medial lateral, and 8 mm ventral). In general, RVLM injection sites were contained within the caudal pole of the facial nucleus to ∼1 mm more caudal, and were ventrally located with respect to the nucleus ambiguous. The location of the tracer was verified histologically (Stern, 2001; Li *et al.* 2003). As previously reported, retrogradely labelled neurones were found in the ventromedial (VM), dorsal cap (DC) and posterior (PaPo) PVN subnuclei (Armstrong *et al.* 1980; Swanson & Sawchenko, 1983; Stern, 2001; Sonner & Stern, 2007).

Hypothalamic slices

Two to three days after the retrograde injection, rats were deeply anaesthetized with nembutal (50 mg kg^{-1}, I.P.), and perfused through the heart with a cold sucrose solution (containing in mM: 200 sucrose, 2.5 KCl, 3 $MgSO_4$, 26 $NaHCO_3$, 1.25 NaH_2PO_4, 20 D-glucose, 0.4 ascorbic acid, 1 $CaCl_2$ and 2 pyruvic acid (290–310 mosmol l^{-1}). Rats were then quickly decapitated, the brains were dissected out, and coronal slices cut (300 μm thick) using a vibroslicer (D.S.K. Microslicer, Ted Pella, Redding, CA, USA). An oxygenated ice cold artificial cerebrospinal fluid (ACSF) was used during slicing (containing in mM: 119 NaCl, 2.5 KCl, 1 $MgSO_4$, 26 $NaHCO_3$, 1.25 NaH_2PO_4, 20 D-glucose, 0.4 ascorbic acid, 2 $CaCl_2$ and 2 pyruvic acid; pH 7.4; 290–310 mosmol l^{-1}). Slices were placed in a holding chamber containing ACSF and kept at room temperature until used (see Stern, 2001 for details).

Electrophysiological recordings

Once in the recoding chamber, slices were bathed with solutions (∼3.0 ml min^{-1}) that were continuously bubbled with 95% O_2–5% CO_2 and maintained at room temperature (∼22–24°C). Patch pipettes (4–7 MΩ) composed of thin walled (1.5 mm outer diameter, 1.17 mm inner diameter) borosilicate glass (GC150T-7.5, Clark, Reading, UK), were pulled on a horizontal electrode puller (P-97, Sutter Instrument Co., Novato, CA, USA). The internal solution contained (mM): 140 potassium gluconate, 0.2 EGTA, 10 Hepes, 10 KCl, 0.9 $MgCl_2$, 4 MgATP, 0.3 NaGTP and 20 sodium phosphocreatine; pH 7.2–7.3. Recordings were obtained with a Multiclamp 700A amplifier (Molecular Devices, Sunnyvale, CA, USA) from fluorescently labelled PVN-RVLM neurons, visualized with a combination of fluorescence illumination and infrared differential interference contrast (IR-DIC) videomicroscopy. The voltage output was digitized at 16-bit resolution, 10 kHz (Digidata 1320A, Molecular Devices), and saved on a computer for offline analysis. Data were discarded if the series resistance (12.8 ± 0.2 MΩ, $n = 106$) was not stable throughout the entire recording. For voltage-clamp recordings, all protocols were run with an output gain of 2, a Bessel filter of 2 kHz, were leak subtracted ($P/4$), and the series resistance was electronically compensated at least 60% throughout the recordings. Data were corrected for the liquid junction potential (6.5 mV), which was experimentally determined using a 2 M KCl agar bridge. For current-clamp recordings, all protocols were run using an output gain of 10 and a Bessel filter of 10 kHz.

Voltage-clamp recordings of I_A and I_T. I_T was pharmacologically isolated using an ACSF containing blockers of voltage-gated sodium and potassium channels. The ACSF contained in mM: 92 NaCl, 2.5 KCl, 1 $MgSO_4$, 26 $NaHCO_3$, 1.25 NaH_2PO_4, 20 D-glucose, 0.4 ascorbic acid, 5 $CaCl_2$, 2 pyruvic acid, 0.5 μM TTX, 30 TEA and 5 4-AP; pH 7.4; 290–310 mosmol l^{-1}). To study the voltage-dependent activation properties of I_T, we used a protocol consisting of a hyperpolarized conditioning pulse (−96.5 mV, 340 ms) followed by a series of depolarizing command pulses (from −76.5 to −26.5 mV, 5 mV increments, 400 ms). At voltages more positive than −20 mV, a slower activating and non-inactivating Ca^{2+} current component (likely to represent high-threshold voltage-activated Ca^{2+} currents, HVA) was generally observed. Thus, to prevent contamination of I_T with HVA Ca^{2+} currents, the maximum command pulse was restricted to −20 mV. I_A was isolated, as previously described (Sonner *et al.* 2007), by using pharmacological methods. In order to block calcium channels, sodium channels and delayed rectifier potassium channels (IK_{DR}), an ACSF with nominal Ca^{2+} (0 mM) was used (containing

in mM: 102 NaCl, 2.5 KCl, 3 $MgSO_4$, 26 $NaHCO_3$, 1.25 NaH_2PO_4, 20 D-glucose, 0.4 ascorbic acid, 2 pyruvic acid, 3 EGTA, 200 μM $CdCl_2$, 0.5 μM TTX and 30 mM TEA; pH 7.4; 290–310 mosmol l^{-1}). The protocol used was the same as above.

In both cases, the normalized peak current amplitudes were plotted as a function of the conditioning step potentials, and fitted with a Boltzmann function, to determine their half-activation potential. I_A and I_T activation thresholds were defined as the membrane potential at which a transient current $\geq$10 pA was detected.

To study the direct interaction between I_A and I_T we selected recording conditions that allowed the detection of both currents simultaneously. For these experiments, we used a modified ACSF containing (in mM): 97 NaCl, 2.5 KCl, 1 $MgSO_4$, 26 $NaHCO_3$, 1.25 NaH_2PO_4, 20 D-glucose, 0.4 ascorbic acid, 5 $CaCl_2$, 2 pyruvic acid, 0.5 μM TTX and 30 TEA; pH 7.4; 290–310 mosmol l^{-1}), and used the same electrophysiological protocol mentioned above. The current density of I_A and I_T was determined by dividing the current amplitude at each command potential by the cell capacitance, obtained by integrating the area under the transient capacitive phase of a 5 mV depolarizing step pulse, in voltage clamp mode. The rate of activation of I_T was determined by measuring the 10–90% rise time from the baseline to the peak of the current at a command pulse of −40 mV. The time constant (τ) of inactivation of I_T was determined by fitting a monoexponential function to the decay phase of the current activated at a command pulse of –40 mV.

Low-threshold spikes. Low-threshold spikes (LTSs) were evoked in current-clamp mode in the presence of TTX. Current was injected to maintain the membrane potentential (V_m) at ∼–90 mV, and the LTSs evoked by injecting depolarizing pulses (20–100 pA, 220 ms). The LTS threshold was obtained by fitting a monoexponential function to the trace and determining the V_m at which the fitted curve no longer fitted the trace.

Spontaneous repetitive firing activity. Spontaneous repetitive firing activity was recorded from PVN-RVLM neurones in continuous mode. The mean firing frequency (2–3 min period) obtained before and after bath application of 100 μM $NiCl_2$ was calculated and compared using Mini Analysis software (Synaptosoft, Fort Lee, NJ, USA). It is known that 4-AP facilitates presynaptic release of neurotransmitter (Flores-Hernandez *et al.* 1994), and thus direct effects of 4-AP on intrinsic properties could be masked by this presynaptic effect. Therefore, all current-clamp experiments were performed in the presence of receptor blockers of the main excitatory (glutamate) and inhibitory (GABA) neurotransmitters in this system. The ACSF used for current-clamp experiments contained (in mM): 110 NaCl, 2.5 KCl, 1 $MgSO_4$, 26 $NaHCO_3$, 1.25 NaH_2PO_4, 20 D-glucose, 0.4 ascorbic acid, 5 $CaCl_2$, 2 pyruvic acid, 0.5 μM TTX, 300 μM picrotoxin and 2 mM kynurenic acid; pH 7.4; 290–310 mosmol l^{-1}).

Confocal calcium imaging

As previously described (Sonner *et al.* 2008), Fluo-5F pentapotassium salt (100 μM; Invitrogen/Molecular Probes, Carlsbad, CA, USA) was incorporated into the internal solution in order to allow for dye-loading into identified PVN-RVLM neurones. Once in the whole-cell mode, the dye was allowed to dialyse into the cell for at least 20 min before the initiation of the recordings, in order to allow complete dialysis of the dye. Calcium imaging was conducted using the Yokogawa real time live cell laser confocal system combined with a highly sensitive EMCCD camera (iXON+885, Andor Technology, South Windsor, CT, USA). Fluorescence images were obtained using diode-pumped solid-state laser (Melles Griot, Carlsbad, CA, USA), and fluorescence emission was collected at >495 nm. Images were acquired at a rate of 40–50 Hz. The fractional fluorescence (F/F_0) was determined by dividing the fluorescence intensity (F) within a region of interest (ROI; 6 × 6 pixels ≈ 4.8 × 4.8 μm) by a baseline fluorescence value (F_0) determined from 30 images before a LTS was evoked (a period showing no change in intracellular calcium levels) (Sonner *et al.* 2008). Between three and four traces of calcium transients evoked by LTS were averaged in order to increase the signal to noise ratio. Data were analysed using Andor IQ software (Andor Technology, Belfast, UK).

Single cell real time, reverse transcription-polymerase chain reaction

To quantitatively assess changes in the expression of Kv4.3 and Cav3.1 K^+ and Ca^{2+} channel subunits, respectively, as well as a to establish correlation between the expression of these channel subunits and the properties of I_A and I_T, we perform single cell real-time PCR from individually recorded PVN-RVLN neurons. For our studies, we have followed quantitative approaches described in details by (Livak & Schmittgen, 2001). A similar approach was recently used in other laboratories to successfully assess mRNA levels within individually identified GnRH neurons (Parhar *et al.* 2003). Briefly, the cytoplasm of a single neurone was gently pulled into a pipette with negative pressure, taking care not to contain the nucleus. The cytoplasm in the pipette was dissipated into a prepared tube containing (in μl) 18 of nuclease free water, 3 of 7× genomic DNA Wipeout Buffer and stored at −70°C. After finishing all recordings, the tubes

Table 1. Primers used in the single cell real time PCR reactions

Gene (accession no.)	Sequence (forward/reverse)		T_m (°C)	Product size (bp)
Kv4.3 (U42975)	5′-AGGCTTCTTCATTGCGGTCT-3′	5′-GTGTCCAGGCAGAAGAAAGC-3′	60	126
Cav3.1 (AF027984)	5′-CAGTGTGTGGGAGATTGTGG-3′	5′-TGTCCATGGTCTTCATGAGC-3′	60	140

were heated to 42°C for 2 min and incubated on ice for at least 1 min. The mixture of (in μl) 6 of 5× Quantiscript RT Buffer, 1 of RT Primer Mix, 1 of Quantiscipt reverse transcriptase was subsequently added and incubated at 42°C for 15 min. The reaction was terminated by heating at 95°C for 3 min and stored at −20°C. All reagents for reverse transcription were purchased from Qiagen (Valencia, CA, USA). Real time PCR amplification was induced by using a fraction of the single cell cDNA as a template. The cDNA of the single neurone was split by 4 μl for three primer sets of glyceraldehyde 3-phosphate dehydrogenase (GAPDH), Kv4.3 and Cav3.1. The reaction mixture (20 μl total volume) contained (in μl): 1 of 25 μM each forward and reverse primer, 4 of nuclease free water and 4 of the cDNA template, 10 of 2× SYBR Green Master Mix (Applied Biosystems, Foster City, CA, US). The annealing temperature in the thermal cycler was 60°C and 50 cycles were performed using an ABI Prism 7700 sequence detector (Applied Biosystems). Quantification was conducted by determining the relative changes in gene expression, to a chosen reference gene, using the $2^{-\Delta\Delta C_t}$ method (Livak & Schmittgen, 2001). Statistical significance was determined by comparing raw ΔC_t values. The standard deviations were used to calculate range values ($2^{-(\Delta\Delta C_t \pm \text{S.D. of } \Delta C_t)}$) for graphs. We compared the efficiency between the target gene (Kv4.3 or Cav3.1) and GAPDH by plotting the ΔC_t *versus* the log of the dilution ratio. The primers were optimized for each reaction, and considered efficient if the absolute value of the slope was less than 1. The slopes of Kv4.3 and Cav3.1 were determined to be 0.07 and 0.005, respectively. All primers used in this study, except GAPDH (purchased from Qiagen, Valencia, CA, USA), were designed by Primer 3 (Whitehead Institute, Cambridge, MA, USA) and synthesized by Bioneer (Alameda, CA, USA). The primer set used in this study is presented in Table 1. The product size was adjusted around 150 bp that is suitable for the real time PCR reaction. Controls used in our studies included harvested neurons that were processed similarly, but without the RT step, as well as buffer without harvested neurons.

Immunohistochemistry

In a subpopulation of recordings, PVN-RVLM neurones were intracellularly filled with biocytin (0.2%) and processed for immunohistochemical detection of oxytocin and vasopressin immunoreactivities. Slices were briefly fixed overnight in a 4% paraformaldehyde–0.2% picric acid solution, dissolved in 0.3 M phosphate buffered saline (PBS; pH ∼7.3) and then thoroughly rinsed with 0.01 M PBS. Slices were then dehydrated using increasing concentrations of ethanol (60–100%; 10% increments; 10 min each step except 100% for 20 min), and then incubated in xylene for 10 min followed by the reverse ethanol procedure (100–60%). Slices were then rinsed in 0.01 M PBS with 0.5% Triton X-100 (TX) for 10 min, and incubated for 45 min in 10% normal horse serum with 0.01 M PBS, 0.5% TX and 0.04% NaN_3. Slices were then thoroughly rinsed with 0.01 M PBS, 0.5% TX and 0.04% NaN_3, followed by a 48 h incubation with a cocktail containing a combination of primary antibodies for oxytocin and vasopressin (both raised in guinea pig, used at 1:50,000 dilution; Bachem, Torrance, CA, USA) in 0.01 M PBS, 0.5% TX and 0.04% NaN_3. Slices were then rinsed in 0.01 M PBS, 0.5% TX and 0.04% NaN_3 for 30 min and then incubated overnight with the secondary antibodies: CY5-streptavidin (1:10,000) and FITC-guinea pig (1:400; both from Jackson ImmunoResearch Laboratories, West Grove, PA, USA) in 0.01 M PBS, 0.5% TX and 0.04% NaN_3. Slices were then thoroughly rinsed in 0.01 M PBS for 20 min, mounted, and visualized using fluorescence microscopy (20×; Olympus America Inc., Melville, NY, USA).

Chemicals

All chemicals were obtained from Sigma-Aldrich (St Louis, MO, USA), with the exceptions of pyruvic acid (MP Biomedicals, Aurora, OH, USA) and TTX (Alomone Labs, Jerusalem, Israel).

Statistical analysis

All values are expressed as means ± S.E.M. In most cases, Student's unpaired or paired *t* test was used, as indicated. Two-way ANOVA with Bonferroni *post hoc* test was used as needed. Pearson's correlation test was used to determine if correlations existed between two parameters. Differences were considered significant at $P < 0.05$. All statistical analyses were conducted using GraphPad Prism (GraphPad Software, San Diego, CA, USA).

Results

Whole-cell patch clamp recordings were obtained from retrogradely labelled PVN-RVLM neurones in sham ($n = 80$) and hypertensive ($n = 90$) rats. The mean input resistance was $1003 \pm 84.0\,M\Omega$ and $1034 \pm 79.2\,M\Omega$ for sham and hypertensive PVN-RVLM neurones, respectively ($P = 0.8$). Neuronal cell capacitance was slightly, though significantly reduced in PVN-RVLM neurones during hypertension (sham: 20.6 ± 1.0 pF; hypertensive: 17.6 ± 0.9 pF, $P < 0.05$), as previously reported (Sonner *et al.* 2008).

Interplay between I_A and I_T within individual PVN-RVLM neurones

In response to depolarizing steps from a hyperpolarized V_m, and under conditions where Ca^{2+} or K^+ currents were pharmacologically isolated, both a transient outward K^+ current (I_A) and a transient inward Ca^{2+} current (I_T) were observed, respectively, in PVN-RVLM neurones (Fig. 1*A*). Both currents were observed over the voltage range tested. Plots of normalized I_A and I_T current amplitude *vs.* command potentials were generated and fitted with a Boltzmann function (Fig. 1*B*). Note that the current–voltage plot for I_T was negatively shifted with respect to I_A. I_T activated at a significantly more hyperpolarized V_m than I_A (mean activation threshold: $I_T = -54.6 \pm 1.6$ mV; $I_A = -46.3 \pm 1.2$ mV, $P = 0.001$, Fig. 1*C*), and the half-activation V_m of I_T was significantly more hyperpolarized than that of I_A (I_T, -40.8 ± 4.0 mV; I_A, -33.1 ± 4.0 mV, ($P < 0.01$). The steepness of the activation curve was not significantly different between I_T an I_A (slope factor, k, for $I_T = 6.0 \pm 1.2$ mV *vs.* $I_A = 7.5 \pm 0.4$; $P = 0.1$).

I_T rise time (10–90%) and $\tau_{inactivation}$ ranged from 3.2 to 25.4 ms (mean rise time $= 14.6 \pm 3.1$ ms) and from 8.4 to 50.6 ms (mean $\tau_{inactivation} = 31.9 \pm 5.5$ ms), respectively, at a command potential of -40 mV ($n = 8$). These values were similar to those we recently reported for I_A (Sonner & Stern, 2007).

As we previously showed (Stern, 2001; Sonner & Stern, 2007), I_A and I_T were sensitive to block by 4-AP (2–5 mM) and $NiCl_2$ (100 μM), respectively (not shown). No differences in current density between I_A and I_T were observed over the voltage range tested ($P = 0.12$, 2-way ANOVA, not shown).

Based on the large overlap in their voltage-dependent and kinetic properties, we investigated whether these currents with opposing polarities interacted at similar membrane potentials. To this end, I_A and I_T were simultaneously recorded in the same PVN-RVLM neurones. Both transient currents were observed in each individually tested neurone ($n = 16$) (Fig. 2). In most cases (13/16), I_T became apparent at a significantly more hyperpolarized V_m than I_A ($I_T = -51.8 \pm 1.9$ mV and $I_A = -36.2 \pm 2.3$ mV; $P < 0.0005$; see also Fig. 2*A* and *B*). As the V_m became more depolarized (-45 through -20 mV), I_A grew in amplitude at a much larger rate than I_T. Thus, at relatively hyperpolarized V_m, a relative dominance of I_T over I_A was observed (~ -50 mV $= I_T$: 48.5 ± 10.1 pA, I_A: 11.0 ± 4.8 pA; $P < 0.05$); the opposite was true at depolarized V_m (~ -25 mV $= I_T$: 92.5 ± 32.3 pA, I_A: 213.7 ± 32.5 pA; $P < 0.05$) (Fig. 2*B* and *C*). The competitive interaction between I_T and I_A was further confirmed by studies showing that pharmacological blockade of I_A (5 mM 4-AP) unmasked a significantly larger I_T (2-way ANOVA, $F = 23.8$, and 38.6, for 4-AP treatment and voltage, respectively, $n = 16$, $P < 0.001$ in both cases, Fig. 2*B*).

In recent studies, we showed that Kv4.3 and Cav3.1 are the K^+ and Ca^{2+} subunits more predominantly expressed in PVN-RVLM neurones (Lee *et al.* 2007; Sonner *et al.*

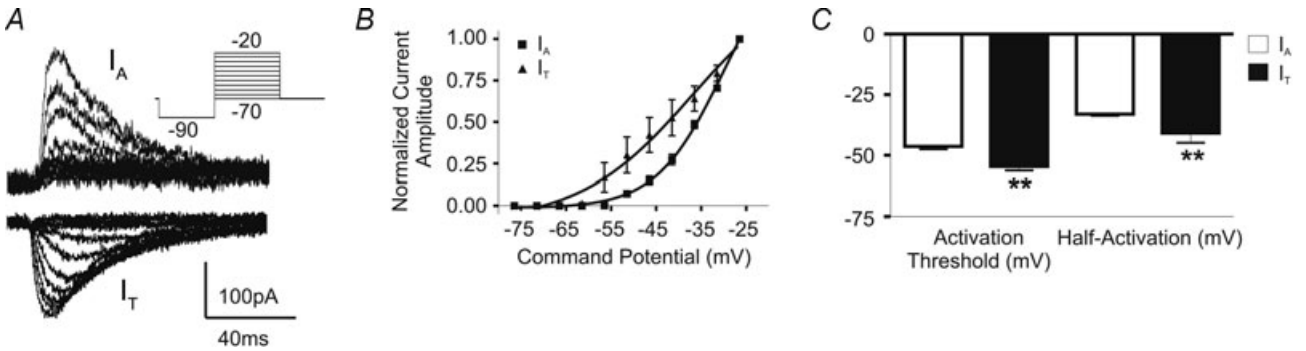

Figure 1. I_A and I_T are expressed in PVN-RVLM neurons
A, representative examples of isolated I_A (upper trace) and I_T (lower trace) in PVN-RVLM neurones. *B*, mean plots of I_A (squares) and I_T (triangles) normalized current amplitudes *vs.* the command potential. Boltzmann functions were fitted to the *I–V* plots. *C*, summary of the activation thresholds and half-activation potentials of I_A and I_T in sham PVN-RVLM neurons. Note the more hyperpolarized activation threshold and half-activation potential for I_T when compared to I_A. $^{**}P < 0.01$. All traces and data shown from sham rats.

2007; Sonner & Stern, 2007), likely to mediate I_A and I_T, respectively. To determine whether the relative expression of these subunits is an important factor influencing the I_T/I_A balance, we simultaneously recorded I_A and I_T in a subset of neurones ($n = 15$, note that for this analysis, data from sham and hypertensive rats were pooled) in which the cytoplasmic content was subsequently aspirated, and the Kv4.3 and Cav3.1 mRNA levels were quantitatively assessed using single-cell real-time RT-PCR (Methods). mRNA levels were quantified using a ΔC_t approach (Methods). Thus, the less Cav3.1 relative to Kv4.3 mRNA expressed within a cell, the larger the ΔC_t Cav3.1/Kv4.3 ratio will be. The ratio of the amplitude of the evoked I_T and I_A at a V_m of ~−20 mV was plotted as a function of the Cav3.1/Kv4.3 subunit expression ratio for that particular neurone (Fig. 3*A*,*B*). As expected, a negative correlation between the I_T/I_A and the ΔC_t Cav3.1/Kv4.3 ratios was observed ($r^2 = 0.61$; $P < 0.001$, Fig. 3*B*).

The I_T /I_A balance influences the expression and magnitude of low threshold spikes (LTS)

It is well established that I_T mediates low threshold spikes (LTS), which promotes bursting firing patterns (Llinas & Yarom, 1981; Stern, 2001). I_A, on the other hand, is known to mediate a transient outward rectification (TOR), delaying spike firing onset (Bourque, 1988; Fisher *et al.* 1998; Luther & Tasker, 2000). Given our results supporting the presence of both opposing transient currents in PVN-RVLM neurones, we aimed to determine whether and how their balance influenced neuronal membrane voltage behaviour. Therefore, we simultaneously recorded I_A and I_T in the voltage-clamp mode, and then determined whether a LTS or a TOR was observed in the current-clamp mode (Methods). In all cases where I_T was more evident than I_A at hyperpolarized command potentials, $n = 40/49$), a LTS was evoked upon membrane depolarization. Conversely, in the few cases where I_A was more evident than at I_T ($n = 9/49$), a TOR was observed (Fig. 4*A*). The differential incidence between LTS/I_T and TOR/I_A was significant ($P < 0.0001$, Fisher's exact test).

We then investigated whether pharmacologically altering the I_T/I_A balance towards an inward current predominance affected the magnitude of the LTS. Thus, LTS properties were analysed before and after application of 5 mM 4-AP ($n = 22$). While the LTS threshold was not affected by I_A blockade ($\Delta = 0.62 \pm 0.65$ mV, $P = 0.9$), both the LTS peak amplitude and area were significantly enhanced during I_A blockade (200.1 ± 18.1%, $P < 0.0005$ and 144.9 ± 16.2%, $P = 0.01$, respectively) (Fig. 4*B* and *C*).

The I_T/I_A balance in PVN-RVLM neurones is dependent on their neurochemical phenotype

Preautonomic PVN neurones, including those innervating the RVLM, are neurochemically heterogeneous, and a proportion of them express the neurohormone vasopressin (VP) or the neurohormone oxytocin (OT)

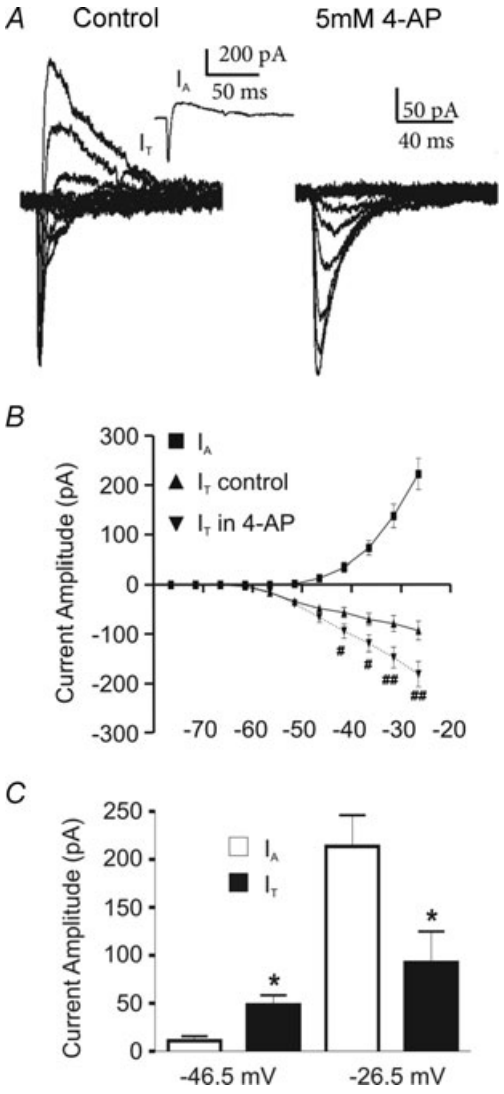

Figure 2. I_A and I_T overlap at similar membrane potentials
A, representative example of a PVN-RVLM neurone in which both I_A and I_T were simultaneously recorded at the same command potentials. Note that when the I_A inhibitor 4-AP was applied, I_A was blocked and I_T became larger in amplitude. Inset, currents evoked at –41.5 mV are shown. *B*, plot of the mean I_A and I_T amplitude *versus* command potential, before and during 4-AP ($n = 16$; I_A control: squares; I_T control: triangles; I_T in 4-AP: inverted triangles). #$P < 0.05$ and ##$P < 0.001$, I_T control *vs.* I_T 4-AP. *C*, summary of current amplitudes of I_A and I_T at a relatively hyperpolarized (–46.5 mV) and a depolarized (–26.5 mV) command potentials. Note that at the hyperpolarized potential the I_T amplitude was larger than that of I_A, whereas the opposite was observed at the more depolarized potential.

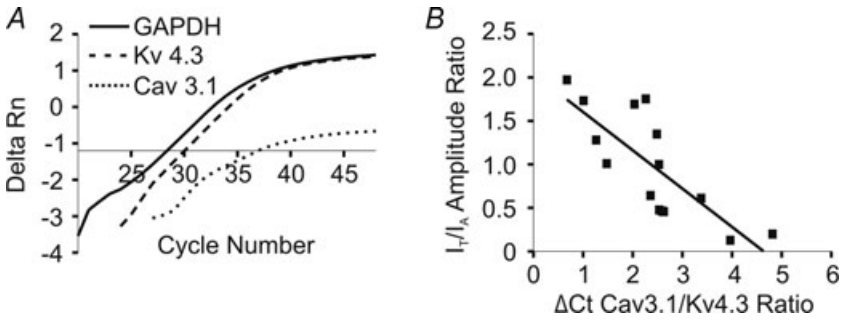

Figure 3. The relative expression of Kv4.3 and Cav3.1 mRNAs correlates with the relative balance between I_A and I_T
A, representative example of real-time PCR amplifications from a single PVN-RVLM neuron from a sham rat, in which the A-type channel subunit Kv4.3 (dashed line) and the T-type channel subunit Cav3.1 (dotted line) mRNAs were tested against the reference gene, GAPDH (continuous line). The cycle numbers that the respective lines crossed the *x*-axis are their threshold values (C_t). Note that Cav3.1 mRNA crossed the *x*-axis at a later cycle number than did Kv4.3, indicating less Cav3.1 mRNA expression compared to Kv4.3. *B*, summary of the relative expression of Cav3.1/Kv4.3 single-cell mRNA compared to the I_T/I_A amplitude ratio measured at –20 mV. Note that the ΔC_t value is used in the plot. Thus, the less Cav3.1 relative to Kv4.3 mRNA expressed, the larger the ΔC_t Cav3.1/Kv4.3 ratio will be. A significant correlation between current amplitude and mRNA expression ratios was observed ($r^2 = 0.61$, $P < 0.001$). For this analysis, neurons from both sham and hypertensive rats were used.

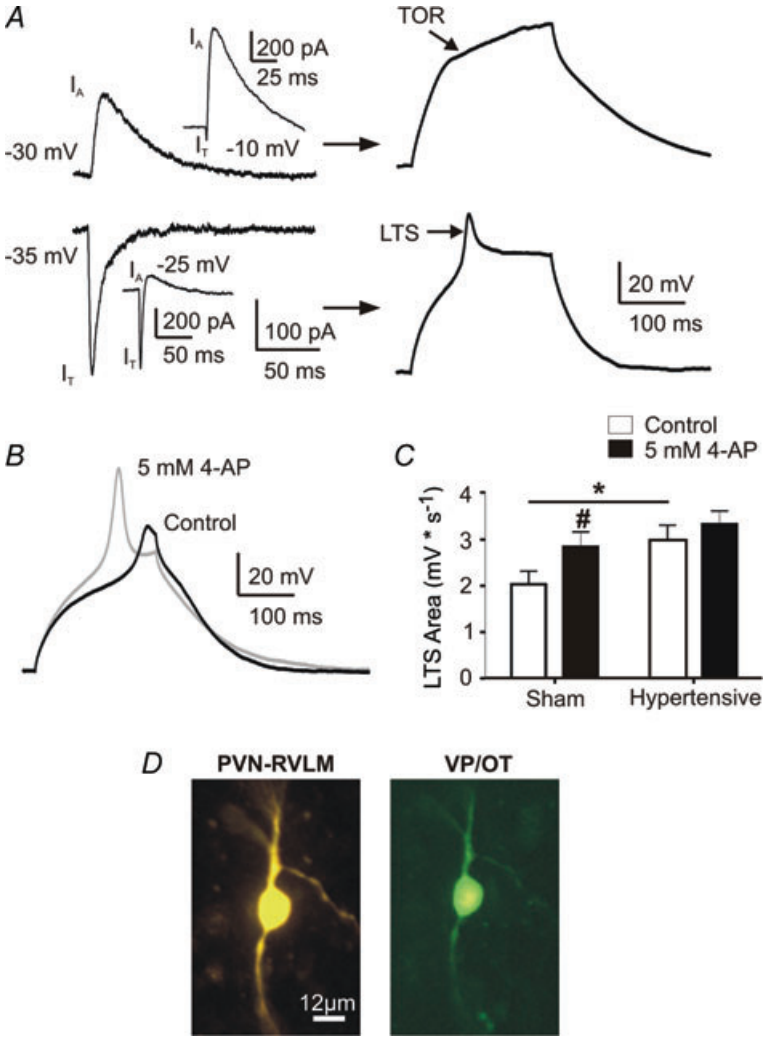

Figure 4. The I_T / I_A balance influences the expression and magnitude of LTSs
A, left, summary data showing that all neurons in which I_T activated at more hyperpolarized potentials than I_A showed a LTS, whereas those in which I_A activated at more hyperpolarized potentials than I_T showed a TOR in response to membrane depolarization. Right, representative traces for each of these conditions are shown (upper panels: more hyperpolarized I_A/TOR; lower panels: more hyperpolarized I_T/LTS). The insets in both cases show the presence of both currents at more depolarized command potentials. *B*, representative example of LTSs before (black) and after (grey) application of the I_A inhibitor 4-AP (5 mM). Note the increased peak and area of the LTS in 4-AP. *C*, summary data of the mea LTS area in PVN-RVLM neurons from sham and hypertensive rats, before and after application of 4-AP. Note that the LTS area was significantly increased in the sham group upon 4-AP application. Also, note the larger basal area in the hypertensive group compared to sham, and the lack of 4-AP effects on the former. *D*, representative photomicrograph (20×) of a PVN-RVLM neuron from a hypertensive rat showing a positive vasopressin/oxytocin (VP/OT) immunoreactivity. #$P < 0.05$ (sham control *vs.* sham 4-AP); *$P < 0.05$ (sham control *vs.* hypertensive control).

(Swanson & Sawchenko, 1983; Yang *et al.* 2001; Mack *et al.* 2002; however, see Stocker *et al.* 2006). Since magnocellular neurosecretory OT and VP neurones of the PVN and SON express a robust I_A and prominent TOR (Fisher *et al.* 1998; Luther & Tasker, 2000), we hypothesized that PVN-RVLM neurones showing a relative dominance of I_A over I_T and a TOR displayed a VP and/or OT phenotype. Therefore, in a subset of recordings ($n = 12$), we simultaneously recorded I_A and I_T in voltage-clamp, and determined whether a TOR or a LTS was observed in current-clamp. Subsequently, the neurochemical phenotype of the recorded neurones was immunohistochemically determined, using a combination of antibodies against oxytocin and vasopressin peptides (Methods, Fig. 4*D*). We found all those neurones in which I_A activated at a more hyperpolarized potential than I_T and displayed TOR were VP/OT immunoreactive ($n = 5/5$) ($P = 0.01$, Fisher's exact test). Conversely, most neurones ($n = 6/7$) in which I_T was evident at a more hyperpolarized potential than I_A and displayed LTS failed to display VP/OT immunoreactivity.

The I_T/I_A balance influences LTS-mediated increases in somatic and dendritic intracellular Ca^{2+} levels

In addition to an increase in membrane conductance and induction of LTS, activation of T-type Ca^{2+} channels also results in changes in intracellular Ca^{2+} levels ($[Ca^{2+}]_i$), and activation of downstream Ca^{2+}-dependent signals (Goldberg *et al.* 2004; Egger *et al.* 2005; Pinato & Midtgaard, 2005). Thus, in order to determine whether the I_T-mediated LTS in PVN-RVLM neurones evoked changes in $[Ca^{2+}]_i$, and whether this was influenced by the I_T/I_A balance, we performed simultaneous patch-clamp recordings and confocal Ca^{2+} imaging. Our results indicate that LTS in PVN-RVLM neurones consistently evoked transient increases in somatic $[Ca^{2+}]_i$ ($n = 13$, Fig. 5). The peak of the Ca^{2+} transient was delayed with respect to the LTS peak (time to peak LTS: 184.3 ± 24.3 ms; time to peak $[Ca^{2+}]_i$: 305.0 ± 49.4 ms, $P = 0.01$), and in all cases, the evoked change in $[Ca^{2+}]_i$ persisted beyond the duration of the LTS (Fig. 5*B*). In general, a correlation between the LTS area and the peak of the Ca^{2+} transient was observed ($r^2 = 0.7$, $P < 0.005$, Fig. 5*C*). The LTS-evoked change in $[Ca^{2+}]_i$ was blocked in nominal 0 Ca^{2+} ACSF, and subthreshold depolarizations failed to evoke a change in $[Ca^{2+}]_i$ (not shown).

When the I_T/I_A balance was pharmacologically shifted towards a predominance of inward currents (5 mM 4-AP), the LTS-evoked change in $[Ca^{2+}]_i$ was significantly enhanced ($P < 0.01$, Fig. 5*D*). On the other hand, the kinetics of the changes in $[Ca^{2+}]_i$ (i.e. rise and decay time courses) were not affected by 4-AP (not shown).

In a few instances, relatively long dendritic processes efficiently loaded with Fluo-5 ($n = 3$) were contained within the same focal plane as the recorded soma. In those cases, we found the somatically evoked LTS to efficiently increase $[Ca^{2+}]_i$ along the dendritic process. As shown in the representative example in Fig. 5*E*, the magnitude of the Ca^{2+} transient increased as a function of the distance from the soma ($P < 0.0001$, 2-way ANOVA), and was significantly enhanced in the presence of 4-AP ($P < 0.001$, 2-way ANOVA) (Fig. 5*F* and *G*). In both cases, changes in $[Ca^{2+}]_i$ along the dendritic process were best fitted by a monoexponential function (control: $r^2 = 0.94$; 4-AP: $r^2 = 0.95$).

A shift in the I_T/I_A balance contributes to enhanced excitability and firing activity in hypertensive rats

Our studies show that a pharmacological shift in the subthreshold balance of I_T/I_A towards a predominance of I_T resulted in enhanced membrane excitability and somatodendritic Ca^{2+} transients. Based on these findings, we explored whether similar changes in the I_T/I_A balance could occur intrinsically in a pathophysiological condition (i.e. renovascular hypertension), and whether such imbalance contributed to aberrant neuronal excitability during this condition. We found I_T current amplitude and density to be enhanced in PVN-RVLM neurones from hypertensive rats ($P < 0.0005$ in both cases, 2-way ANOVA, Fig. 6*A*). No differences in I_T voltage-dependent activation properties or kinetic properties were observed between sham and hypertensive rats (not shown). Along with our recent studies showing a diminished I_A availability in these neurones during hypertension (Sonner *et al.* 2008), these results altogether support a shift in the I_T/I_A balance towards a predominance of I_T in hypertensive rats.

In agreement with diminished I_A and enhanced I_T magnitudes, results from single-cell RT-PCR studies in identified PVN-RVLM neurones from control and hypertensive rats ($n = 20$ and 31 neurones in each group, respectively) indicated a robust reduction in the relative expression levels of Kv4.3 mRNA, and an increase relative expression of Cav3.1 mRNA in hypertensive when compared to sham rats ($P < 0.05$ in both cases) (Fig. 6*B* and *C*). In fact, a nearly 15-fold decrease in the relative expression of Kv4.3 to Cav3.1 mRNA within individual PVN-RVLM neurones was observed in hypertensive, when compared to sham rats ($P < 0.0001$).

The magnitude of the evoked LTS was significantly larger in PVN-RVLM neurones from hypertensive ($n = 24$) when compared to control rats ($P < 0.05$, Fig. 4*C*). Moreover, blockade of I_A in hypertensive rats, in contrast to what was observed in controls, failed to further increase the LTS magnitude ($3.3 \pm 8.1\%$, $P = 0.4$)

(Fig. 4*C*). Likewise, the magnitude of the LTS-evoked change in $[Ca^{2+}]_i$ was significantly larger in PVN-RVLM neurones from hypertensive ($n = 11$) when compared to control rats ($P < 0.05$, Fig. 5*D*), and blockade of I_A in hypertensive rats failed to further increase the magnitude of the evoked Ca^{2+} transient ($P > 0.1$, Fig. 5*D*). Taken together, these results support an imbalanced I_T/I_A relationship during hypertension, resulting in an enhanced LTS and associated changes in $[Ca^{2+}]_i$.

Since I_T has been shown to regulate spontaneous activity in a variety of CNS neurones (Huguenard, 1996; Raman & Bean, 1999), we addressed whether the sub-threshold I_T/I_A imbalance resulted in and/or contributed to increased PVN-RVLM firing activity in hypertensive rats. All recorded neurons in control and hypertensive rats were spontaneously active. However, PVN-RVLM basal spontaneous firing frequency was significantly higher in hypertensive when compared to control rats ($n = 8$ and 12, respectively, $P < 0.05$) (Fig. 7). Bath application of $NiCl_2$ (100 μM), which at this concentration more efficiently blocks I_T over high threshold voltage-activated Ca^{2+} currents (Fox *et al.* 1987; Narahashi *et al.* 1987; Hagiwara *et al.* 1988; Gu & Spitzer, 1993), failed to affect firing discharge in control rats ($P = 0.4$). On the other hand, the firing rate in neurones from hypertensive rats was significantly reduced in the presence of $NiCl_2$ ($P < 0.005$), to a value not significantly different from that observed in control rats ($P > 0.4$). These results support an enhanced I_T contribution to spontaneous firing activity in PVN-RVLM neurones from hypertensive rats.

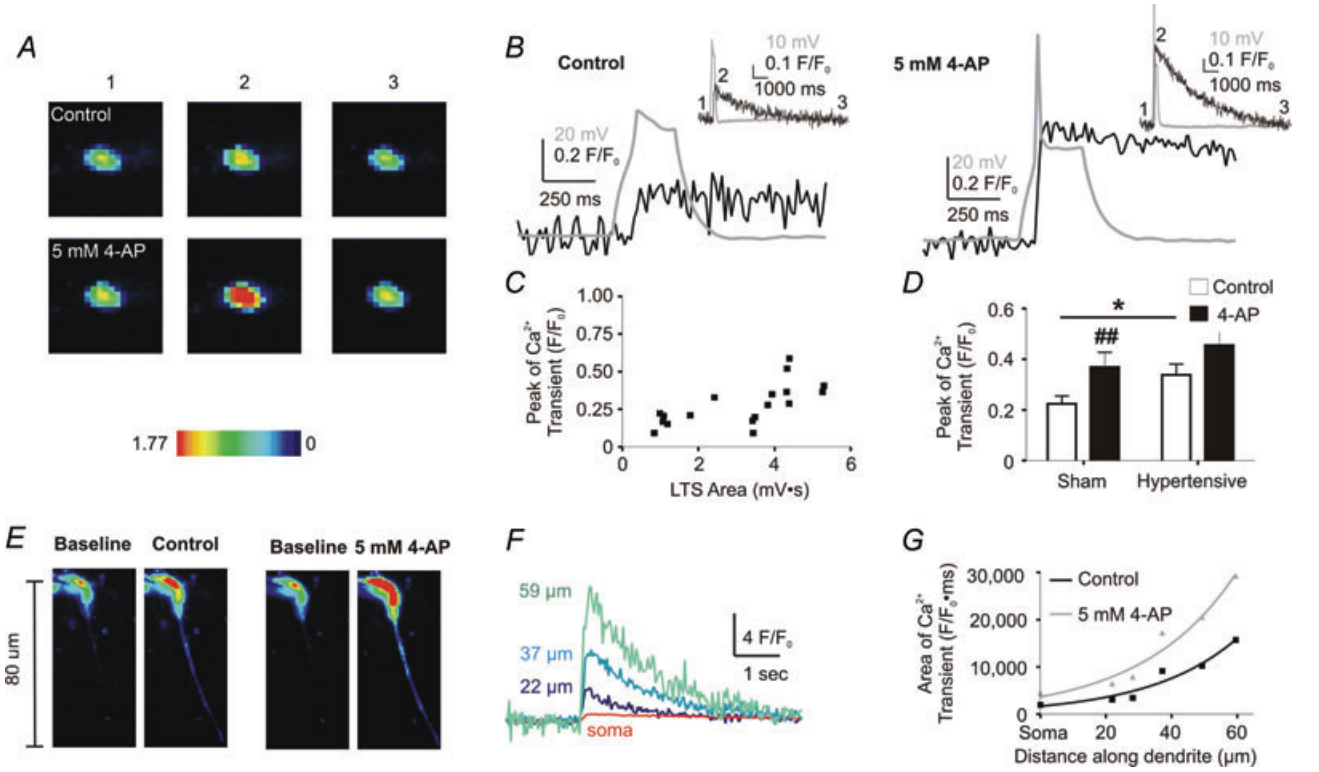

Figure 5. I_A modulates LTS-mediated changes in intracellular Ca^{2+}
A, representative confocal images of LTS-mediated changes in somatic $[Ca^{2+}]_i$ (pseudocolour) in a PVN-RVLM neuron from a sham rat, before and after 4-AP application. Images of the basal $[Ca^{2+}]_i$ (1), maximum peaks (2) and subsequent return to basal levels (3) are displayed (scale units are F/F_0). *B*, representative examples of an evoked LTS (grey) and the resulting change in $[Ca^{2+}]_i$ (black), before (left) and after 4-AP application (right). Inset, same traces shown at a more expanded time scale. Note that the numbers correspond to the images shown in *A*. *C*, plot showing the relationship of the LTS area and the peak of the LTS-evoked Ca^{2+} transient. A significant positive correlation was observed ($r^2 = 0.7$, $P < 0.005$). Neurons from sham and hypertensive control rats were plotted together. *D*, summary data of the mean peak of the Ca^{2+} transient from PVN-RVLM neurons in sham and hypertensive PVN-RVLM rats, before and after 4-AP application. ##$P < 0.01$ (sham control *vs.* sham 4-AP); *$P < 0.05$ (sham control *vs.* hypertensive control). *E*, representative confocal images (pseudocolour) of dendritic, LTS-mediated changes in $[Ca^{2+}]_i$ before and after 4-AP application. *F*, representative traces of Ca^{2+} transients measured at various dendritic distances from the soma of the neuron in *A*. Note that the magnitude of the Ca^{2+} transient increased as a function of the distance from the soma. *G*, summary plot of the area of the Ca^{2+} transient along the dendritic process, before and after addition of 4-AP. Distances measured along the dendrites were binned in tens of micrometres.

Discussion

The main findings that emerge from our studies can be summarized as follows: (a) the subthreshold currents I_A and I_T are both present in PVN-RVLM neurones, and display overlapping voltage-dependent and kinetic properties; (b) The relative predominance of each current at hyperpolarized membrane potentials dictates the membrane behaviour upon depolarization (i.e. expression of LTS or TOR); (c) The I_T/I_A balance within individual neurones correlated with the relative expression of Cav3.1 and Kv4.3 mRNA within the same neurone; (c) pharmacological blockade of I_A unmasked a larger I_T, resulting in an enhanced I_T-mediated LTS as well as LTS-mediated somatodendritic Ca^{2+} transients; (d) in hypertensive rats, there is a shift in the I_T/I_A balance towards an I_T predominance – this shift is in part mediated by a diminished and enhanced Kv4.3 and Cav3.1 mRNA subunit expression, respectively, and the imbalanced I_T/I_A relationship results in an enhanced LTS, LTS-mediated somatodendritic Ca^{2+} transients, and overall increased PVN-RVLM firing activity in hypertensive rats.

Taken together, our results support that a balanced relationship between I_A and I_T influences membrane excitability and Ca^{2+} dynamics in PVN-RVLM neurones. Moreover, an imbalanced interaction between these two opposing currents, favouring I_T, results in enhanced neuronal excitability and firing discharge in hypertensive rats, constituting thus an important underlying mechanism contributing to the characteristic sympathoexcitation observed in this disease.

Interplay between I_A and I_T within individual PVN-RVLM neurones

I_A and I_T are critical inhibitory and excitatory conductances regulating the degree and pattern of spiking activity in the CNS (Segal *et al.* 1984; Rogawski, 1985; Rudy, 1988; McCobb & Beam, 1991; Raman & Bean, 1999; Stern, 2001). In the PVN, both have been shown to play important roles in influencing neuroendocrine and preautonomic neurones. Elegant work by Tasker and colleagues showed that while both I_A and I_T are present in magnocellular and parvocellular neuronal types, differences in their relative expression and voltage-dependent properties determine the distinctive membrane properties in these functionally distinct neuronal populations. Thus, magnocellular neurones predominantly express an I_A-mediated transient outward

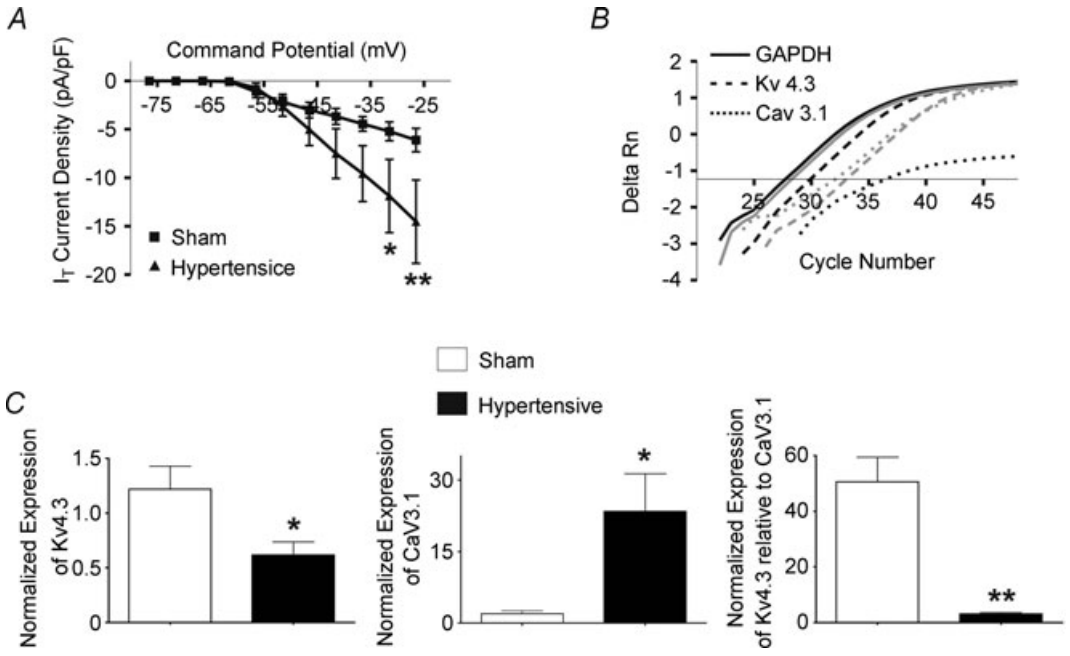

Figure 6. Altered I_T current magnitude, Cav3.1 and Kv4.3 subunits mRNA expression in PVN-RVLM neurons during hypertension
A, mean plots of I_T current densities in PVN-RVLM neurons from sham (squares) and hypertensive (triangles) rats. *B*, representative examples of single-cell, real-time PCR amplifications for Kv4.3 (dashed line), Cav3.1 (dotted line) and GAPDH (whole line) obtained from a PVN-RVLM neuron in sham rat (black) and a PVN-RVLM neuron in a hypertensive rat (grey). *C*, summary data of the normalized expression of single-cell Kv4.3 mRNA (left) and single-cell Cav3.1 mRNA (middle). The normalized expression of Kv4.3 relative to Cav3.1 within individual cells is displayed in the right panel. Note that the expression of Kv4.3 mRNA was reduced while Cav3.1 mRNA expression was enhanced in neurons from hypertensive rats. Also, note the significant reduction in the relative expression of Kv4.3 to Cav3.1 within individual neurons during hypertension. $^*P < 0.05$, $^{**}P < 0.0001$.

rectification (TOR) (Bourque & Renaud, 1991; Stern & Armstrong, 1995; Luther & Tasker, 2000), whereas parvocellular neurones express an I_T-dependent LTS (Luther & Tasker, 2000). In line with these studies, we reported PVN-RVLM neurones to also express both types of subthreshold conductances (Stern, 2001; Sonner & Stern, 2006). Thus, whereas I_T mediates LTS and promotes bursting firing activity, we found I_A to regulate action potential waveform and interspike interval in PVN-RVLM neurones. However, whether and how these two opposing conductances interact with each other, and what the impact of such interplay is on membrane excitability in presympathetic PVN neurones, has not been established. To this end, we simultaneously measured I_A and I_T in identified PVN-RVLM neurones, and evaluated how their interactions influenced basic membrane properties, intracellular Ca^{2+} dynamics and firing activity, under both physiological and pathological conditions.

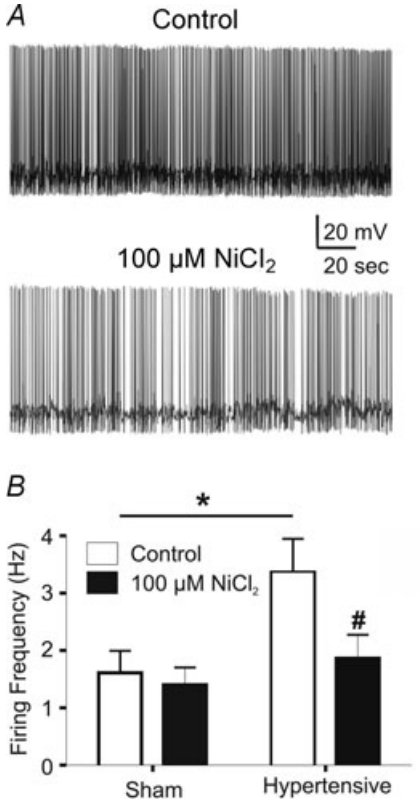

Figure 7. I_T contributes to enhanced PVN-RVLM firing activity in hypertensive rats
A, representative traces of spontaneous firing activity in a PVN-RVLM neuron from a hypertensive rat, before and after addition of 100 μM $NiCl_2$. *B*, summary data of mean spontaneous firing activity in PVN-RVLM neurons from sham and hypertensive rats before and after $NiCl_2$ application. #$P < 0.05$ (hypertensive control *vs.* hypertensive $NiCl_2$); *$P < 0.05$ (sham control *vs.* hypertensive control).

Our results support an active interplay between I_A and I_T in presympathetic PVN neurones. Firstly, both currents displayed overlapping voltage-dependent and kinetic properties. Secondly, pharmacological block of I_A unmasked and/or increased I_T magnitude, resulting in turn in larger and prolonged I_T-mediated LTS, as well as larger LTS-mediated somatodendritic Ca^{2+} transients. In a recent study, 4-AP at the concentration used in this study, was reported to directly potentiated high threshold voltage-dependent Ca^{2+} currents in acutely dissociated spinal cord neurons (Wu *et al.* 2009). On the other hand, low-threshold T-type currents were unaffected. Thus, it is unlikely that the enhanced I_T and the associated LTS reported in our study resulted from a direct action of 4-AP on the T-type channels. Taken together, these results suggest that I_A and I_T can precisely influence each other's availability over a voltage-range near spike threshold, in a way that, for example, diminished or absent I_A will result in the additional recruitment of I_T, and consequently a stronger depolarizing drive and increased probability for action potential firing. These results are in agreement with studies in other CNS areas (Pape *et al.* 1994; Meis *et al.* 1996; Cavelier *et al.* 2003; Molineux *et al.* 2005).

In the majority of PVN-RVLM neurones (81%), and in response to depolarizing steps, I_T became evident at a more hyperpolarized membrane potential than I_A. This pattern corresponded with the predominant and/or exclusive expression of a LTS. Conversely, in the rest of the neurones, I_A became evident before I_T, which corresponded with the expression of a TOR, rather than a LTS. Thus, the relative predominance of I_T over I_A at hyperpolarized membrane potentials seems to strongly influence whether a LTS or a TOR is expressed in PVN-RVLM neurones. Numerous factors could influence the balance or predominance of one conductance over the other. Firstly, it has been suggested that differences in activation threshold can shift the balance between I_A and I_T (Pape *et al.* 1994). Our results show that in the majority of cells, I_T activates at a more hyperpolarized potential than I_A, which may account for the larger proportion of cells expressing LTS that we observed. Secondly, we found a positive correlation between the relative expression of Cav3.1/Kv4.3 mRNA subunits and I_T/I_A amplitude within single cells. Thus, it could be argued that differences in the relative expression and densities of channels underlying I_T and I_A may influence the ability of PVN-RVLM neurones to express an excitatory (LTS) or inhibitory (TOR) membrane behaviour. Finally, another factor that could influence the I_T/I_A balance is the relative distribution of the underlying channels along the somatodendritic plasma membrane. While numerous studies support a heterogeneous distribution of Ca^{2+} and K^+ channels along dendritic trees in various neuronal types (Magee & Johnston, 2005; Nusser, 2009), no information is

currently available on topographical distribution of active conductances in PVN-RVLM neurones.

Importantly, we found the I_T/I_A balance and its impact on membrane properties to be in part dependent on, or correspondent to, the neurochemical phenotype of PVN-RVLM neurones. Preautonomic PVN neurones are known to be neurochemically heterogeneous, with a proportion of them expressing the neuropeptides OT or VP (Swanson & Sawchenko, 1983; Yang *et al.* 2001; Mack *et al.* 2002). Surprisingly, our studies indicate that the majority of PVN-RVLM neurones in which I_A activated at a more hyperpolarized V_m than I_T, and expressed TOR, were immunoreactive for VP/OT. Given the well-established presence of I_A and TOR in magnocellular neurosecretory neurones (Armstrong & Stern, 1998*a*,*b*; Fisher *et al.* 1998; Luther & Tasker, 2000), it seems that OT and VP neurones in the SON and PVN, regardless of their functional roles (i.e. presympathetic or neurosecretory), share a similar I_T/I_A balance and membrane properties.

Functional implications of I_T/I_A interplay in PVN-RVLM neurones

In addition to dictating whether a LTS or a TOR is expressed upon membrane depolarization, subtle changes in the I_T/I_A balance may affect the magnitude of these membrane properties. Thus, as previously demonstrated in thalamic neurones of the lateral geniculate nucleus (Pape *et al.* 1994), we found pharmacological blockade of I_A to significantly amplify and/or prolong the I_T-dependent LTS magnitude.

Our results also suggest that in addition to affecting membrane potential and firing patterns (i.e. tonic and bursting) (Stern, 2001; Lee *et al.* 2008), the LTS also influences somatic and dendritic Ca^{2+} dynamics in PVN-RVLM. This is indicated by our results showing that the LTS, even in the absence of functional Na^+ channels, is sufficient to induce an increase in $[Ca^{2+}]_i$, which can propagate along neuronal dendrites. A similar phenomenon was recently reported in olfactory bulb granule cells and in cortical interneurones (Goldberg *et al.* 2004; Egger *et al.* 2005). We found the magnitude of the dendritic LTS-evoked Ca^{2+} transient to increase as a function of the distance from the soma. A possible interpretation is that I_T channels underlying the LTS are expressed at increasingly higher densities along the dendritic trees, as observed in other CNS bursting neurones (Destexhe *et al.* 1998; Sherman, 2001; Goldberg *et al.* 2004). Alternatively, our results could be confounded by a progressive decrease in dendritic volume with distance from the soma, which is expected to result in an enhanced Ca^{2+} transient (Komendantov *et al.* 2007).

Importantly, we found pharmacological blockade of I_A to result in larger LTS-mediated Ca^{2+} transients, in both somata and dendrites of PVN-RVLM. These results suggest that I_A plays an important role in antagonizing LTS-dependent Ca^{2+} signalling in these neurones. A similar LTS-mediated Ca^{2+} signalling has been shown to be important for boosting distal synaptic inputs (Goldberg *et al.* 2004) and for lateral inhibition in the olfactory bulb (Egger *et al.* 2005). While the functional significance of the LTS-mediated Ca^{2+} signalling in PVN-RVLM neurones is at present unclear, our studies suggest that through this mechanism, these neurones have at least the potential for a subthreshold form of associative plasticity, in which the efficacy of incoming dendritic synaptic inputs may be influenced by recent neuronal activity.

Taken together, our results support that in PVN-RVLM neurones, I_A and I_T act in a concerted manner to regulate subthreshold membrane excitability, action potential firing degree/pattern, as well as somatic and dendritic intracellular Ca^{2+} dynamics. Moreover, they suggest that a diminished I_A availability, as a result of a pharmacological blockade, or alternatively, during a pathological condition, could shift the I_T/I_A balance towards a predominance of I_T, resulting in an overall enhanced excitatory drive

Altered I_T/I_A balance contributes to increased neuronal activity in hypertensive rats

Sympathoexcitation of a central origin is characteristic of hypertension (Judy *et al.* 1976; Guyenet, 2006), and mounting evidence supports an important role for the PVN in enhanced sympathetic outflow in this disease (Earle *et al.* 1992; Earle & Pittman, 1995; Jung *et al.* 2004). Moreover, increased neuronal excitability, associated with elevated blood pressure and sympathetic activity, has recently been demonstrated in PVN-RVLM neurones (Allen, 2002; Li & Pan, 2006). While alterations in various PVN neurotransmitter systems have been reported during hypertension (Petty & Reid, 1977; Martin & Haywood, 1998; Haywood *et al.* 2001; Jung *et al.* 2004), the contribution of altered intrinsic membrane properties to PVN neuronal hyperactivity, during hypertension, remains less investigated. In a recent study, we demonstrated an overall reduction in the magnitude of I_A in PVN-RVLM neurones in renovascular hypertensive rats, which contributed to their enhanced excitability in this condition (Sonner *et al.* 2008). In addition to the previously demonstrated enhanced voltage-dependent inactivation and diminished single channel conductance, our present studies support a diminished expression of Kv4.3 mRNA, the most abundant subunit expressed in PVN-RVLM neurones (Sonner & Stern, 2007), as another contributing factor to blunted I_A function in PVN-RVLM neurones during hypertension.

Importantly, we found in the present study the current amplitude and density of I_T to be enhanced during hypertension. Moreover, expression of Cav3.1 mRNA, the subunit underlying I_T and LTS in PVN neurones (Lee *et al.* 2008), was elevated in PVN-RVLM neurones in hypertensive rats. Thus, a diminished I_A along with an increased I_T magnitude indicates a shift in the I_T/I_A balance towards an inward current predominance during hypertension. This is supported by our results showing an augmented magnitude of the I_T-mediated LTS, as well as the LTS-mediated increase in intracellular Ca^{2+} levels in PVN-RVLM neurones in hypertensive rats. The blunted effect of 4-AP on the LTS and LTS-mediated changes in intracellular Ca^{2+} levels in hypertensive rats supports a contribution of the diminished I_A to the I_T predominance in this condition. Finally, a shift in the I_T/I_A balance in hypertensive rats is supported by our single-cell RT-PCR studies, showing that the relative expression of Kv4.3 to Cav3.1 mRNA in a given cell was significantly reduced during hypertension, shifting from a Kv4.3 predominance towards an equal relative expression of both subunits.

In addition to mediating LTSs, I_T has been shown to regulate spontaneous firing activity in some CNS neurones (Huguenard, 1996; Raman & Bean, 1999). Thus, we aimed to determine whether the shift in the I_T/I_A balance towards an I_T predominance contributed to an enhanced ongoing firing discharge of PVN-RVLM neurones during hypertension (Allen, 2002; Li & Pan, 2006; Sonner *et al.* 2008). Our studies indicate that in hypertensive rats, the basal spontaneous firing activity in PVN-RVLM neurones was significantly increased when compared to sham rats. Moreover, a low concentration of $NiCl_2$ (100 μM), which more selectively blocks I_T over high-threshold voltage-dependent Ca^{2+} channels (Fox *et al.* 1987; Gu & Spitzer, 1993), significantly reduced PVN-RVLM firing activity in hypertensive rats, to levels observed in sham rats. Conversely, $NiCl_2$ had no effect on PVN-RVLM firing discharge in sham rats. Taken together, these results support that under normal conditions, I_T does not contribute to ongoing PVN-RVLM firing activity. On the other hand, the I_T/I_A imbalance in hypertensive rats resulted in a larger I_T predominance, contributing in turn to the elevated spontaneous firing activity observed in this condition. A similar I_T/I_A imbalance was shown to contribute to altered neuronal activity in epileptic conditions (Meis *et al.* 1996). While low micromolar $NiCl_2$ concentations more selectively blocks I_T over high-threshold voltage-dependent Ca^{2+} channels (Fox *et al.* 1987; Narahashi *et al.* 1987; Hagiwara *et al.* 1988; Gu & Spitzer, 1993), the R-type high threshold voltage-gated Ca^{2+} current could have also be affected by $NiCl_2$ (Lee *et al.* 1999). Thus, while R-type currents have not yet been reported in PVN neurons, we cannot completely rule out their involvement in the $NiCl_2$ effects reported here.

It is important to take into consideration that, given the absence of peripheral afferent inputs in the slice preparation, the reported firing activities in these studies reflect only the actions of intrinsic properties and local synaptic inputs preserved in this *in vitro* preparation. Nonetheless, the reported changes in intrinsic neuronal properties reported here are expected to also affect neuronal responsiveness to activation of such afferent inputs.

The underlying mechanisms leading to the I_T/I_A imbalance reported here are at present unknown. Angiotensin II (AngII), however, stands as a likely candidate. Within the PVN, AngII has been shown to increase sympathetic activity (Chen & Toney, 2001; Li *et al.* 2006), and abundant evidence supports enhanced PVN AngII activity during hypertension (Gutkind *et al.* 1988; Jung *et al.* 2004). Importantly, AngII has been shown to inhibit I_A (Nagatomo *et al.* 1995; Li & Ferguson, 1996; Wang *et al.* 1997) and to enhance the I_T-dependent LTS activity (Spanswick & Renaud, 2005). Moreover, AngII has been shown to diminish I_A current amplitude and diminish Kv4.3 mRNA in the RVLM of rats with congestive heart failure (Gao *et al.* 2006). Thus, future studies evaluating the contribution of AngII to altered I_T/I_A balance in PVN-RVLM neurones during hypertension are warranted.

In summary, our results support a dynamic interplay between the subthreshold currents I_A and I_T in the control of PVN-RVLM membrane properties, firing activity and intracellular Ca^{2+} dynamics. Moreover, our studies support an imbalanced I_T/I_A interplay, favouring I_T, to contribute to increased neuronal excitability and firing discharge in PVN-RVLM neurones in renovascular hypertensive rats.

References

Allen AM (2002). Inhibition of the hypothalamic paraventricular nucleus in spontaneously hypertensive rats dramatically reduces sympathetic vasomotor tone. *Hypertension* **39**, 275–280.

Armstrong WE & Stern JE (1998*a*). Electrophysiological distinctions between oxytocin and vasopressin neurons in the supraoptic nucleus. *Adv Exp Med Biol* **449**, 67–77.

Armstrong WE & Stern JE (1998*b*). Phenotypic and state-dependent expression of the electrical and morphological properties of oxytocin and vasopressin neurones. *Prog Brain Res* **119**, 101–113.

Armstrong WE, Warach S, Hatton GI & McNeill TH (1980). Subnuclei in the rat hypothalamic paraventricular nucleus: a cytoarchitectural, horseradish peroxidase and immunocytochemical analysis. *Neuroscience* **5**, 1931–1958.

Bergamaschi C, Campos RR, Schor N & Lopes OU (1995). Role of the rostral ventrolateral medulla in maintenance of blood pressure in rats with Goldblatt hypertension. *Hypertension* **26**, 1117–1120.

Bourque CW (1988). Transient calcium-dependent potassium current in magnocellular neurosecretory cells of the rat supraoptic nucleus. *J Physiol* **397**, 331–347.

Bourque CW & Renaud LP (1991). Membrane properties of rat magnocellular neuroendocrine cells in vivo. *Brain Res* **540**, 349–352.

Carvalho TH, Bergamaschi CT, Lopes OU & Campos RR (2003). Role of endogenous angiotensin II on glutamatergic actions in the rostral ventrolateral medulla in Goldblatt hypertensive rats. *Hypertension* **42**, 707–712.

Cavelier P, Desplantez T, Beekenkamp H & Bossu JL (2003). K^+ channel activation and low-threshold Ca^{2+} spike of rat cerebellar Purkinje cells in vitro. *Neuroreport* **14**, 167–171.

Ciriello J, Caverson MM & Calaresu FR (1985). Lateral hypothalamic and peripheral cardiovascular afferent inputs to ventrolateral medullary neurons. *Brain Res* **347**, 173–176.

Chen QH & Toney GM (2001). AT_1-receptor blockade in the hypothalamic PVN reduces central hyperosmolality-induced renal sympathoexcitation. *Am J Phyiol Regul Integr Comp Physiol* **281**, R1844–1853.

Coote JH, Yang Z, Pyner S & Deering J (1998). Control of sympathetic outflows by the hypothalamic paraventricular nucleus. *Clin Exp Pharmacol Physiol* **25**, 461–463.

Dampney RA, Czachurski J, Dembowsky K, Goodchild AK & Seller H (1987). Afferent connections and spinal projections of the pressor region in the rostral ventrolateral medulla of the cat. *J Auton Nerv Syst* **20**, 73–86.

Dampney RA, Horiuchi J, Killinger S, Sheriff MJ, Tan PS & McDowall LM (2005). Long-term regulation of arterial blood pressure by hypothalamic nuclei: some critical questions. *Clin Exp Pharmacol Physiol* **32**, 419–425.

Destexhe A, Neubig M, Ulrich D & Huguenard J (1998). Dendritic low-threshold calcium currents in thalamic relay cells. *J Neurosci* **18**, 3574–3588.

Drummond GB (2009). Reporting ethical matters in *The Journal of Physiology*: standards and advice. *J Physiol* **587**, 713–719.

Earle ML, Boorman R, Takahashi Y & Pittman QJ (1992). Lesions of the paraventricular nucleus alter the development and intensity of chronic renal hypertension. *Can J Physiol Pharmacol* **70**, Avii–Aviii.

Earle ML & Pittman QJ (1995). Involvement of the PVN and BST in 1K1C hypertension in the rat. *Brain Res* **669**, 41–47.

Egger V, Svoboda K & Mainen ZF (2005). Dendrodendritic synaptic signals in olfactory bulb granule cells: local spine boost and global low-threshold spike. *J Neurosci* **25**, 3521–3530.

Esler M & Kaye D (1998). Increased sympathetic nervous system activity and its therapeutic reduction in arterial hypertension, portal hypertension and heart failure. *J Auton Nerv Syst* **72**, 210–219.

Fisher TE, Voisin DL & Bourque CW (1998). Density of transient K^+ current influences excitability in acutely isolated vasopressin and oxytocin neurones of rat hypothalamus. *J Physiol* **511**, 423–432.

Flores-Hernandez J, Galarraga E, Pineda JC & Bargas J (1994). Patterns of excitatory and inhibitory synaptic transmission in the rat neostriatum as revealed by 4-AP. *J Neurophysiol* **72**, 2246–2256.

Fox AP, Nowycky MC & Tsien RW (1987). Kinetic and pharmacological properties distinguishing three types of calcium currents in chick sensory neurones. *J Physiol* **394**, 149–172.

Gao L, Wang W, Mann E, Finch M, Li Y, Liu D, Schultz HD & Zucker IH (2006). Sympathoexcitation in chronic heart failure: AngII induced inhibition of voltage-gated K^+ channel, an in vivo and in vitro study. *FASEB J* **20**, A1202–A1203.

Goldberg JH, Lacefield CO & Yuste R (2004). Global dendritic calcium spikes in mouse layer 5 low threshold spiking interneurones: implications for control of pyramidal cell bursting. *J Physiol* **558**, 465–478.

Gu X & Spitzer NC (1993). Low-threshold Ca^{2+} current and its role in spontaneous elevations of intracellular Ca^{2+} in developing *Xenopus* neurons. *J Neurosci* **13**, 4936–4948.

Gutkind JS, Kurihara M, Castren E & Saavedra JM (1988). Increased concentration of angiotensin II binding sites in selected brain areas of spontaneously hypertensive rats. *J Hypertens* **6**, 79–84.

Guyenet PG (2006). The sympathetic control of blood pressure. *Nat Rev Neurosci* **7**, 335–346.

Hagiwara N, Irisawa H & Kameyama M (1988). Contribution of two types of calcium currents to the pacemaker potentials of rabbit sino-atrial node cells. *J Physiol* **395**, 233–253.

Hardy SG (2001). Hypothalamic projections to cardiovascular centers of the medulla. *Brain Res* **894**, 233–240.

Haywood JR, Mifflin SW, Craig T, Calderon A, Hensler JG & Hinojosa-Laborde C (2001). γ-Aminobutyric acid (GABA)-A function and binding in the paraventricular nucleus of the hypothalamus in chronic renal-wrap hypertension. *Hypertension* **37**, 614–618.

Hosoya Y, Sugiura Y, Okado N, Loewy AD & Kohno K (1991). Descending input from the hypothalamic paraventricular nucleus to sympathetic preganglionic neurons in the rat. *Exp Brain Res* **85**, 10–20.

Huguenard JR (1996). Low-threshold calcium currents in central nervous system neurons. *Annu Rev Physiol* **58**, 329–348.

Judy WV, Watanabe AM, Henry DP, Besch HR Jr, Murphy WR & Hockel GM (1976). Sympathetic nerve activity: role in regulation of blood pressure in the spontaenously hypertensive rat. *Circ Res* **38**, 21–29.

Jung JY, Lee JU & Kim WJ (2004). Enhanced activity of central adrenergic neurons in two-kidney, one clip hypertension in Sprague-Dawley rats. *Neurosci Lett* **369**, 14–18.

Komendantov AO, Trayanova NA & Tasker JG (2007). Somato-dendritic mechanisms underlying the electrophysiological properties of hypothalamic magnocellular neuroendocrine cells: a multicompartmental model study. *J Comput Neurosci* **23**, 143–168.

Kubo T, Hagiwara Y, Sekiya D, Chiba S & Fukumori R (2000). Cholinergic inputs to rostral ventrolateral medulla pressor neurons from hypothalamus. *Brain Res Bull* **53**, 275–282.

Lambert RC, McKenna F, Maulet Y, Talley EM, Bayliss DA, Cribbs LL, Lee JH, Perez-Reyes E & Feltz A (1998). Low-voltage-activated Ca^{2+} currents are generated by members of the CavT subunit family ($\alpha_{1G/H}$) in rat primary sensory neurons. *J Neurosci* **18**, 8605–8613.

Lee JH, Gomora JC, Cribbs LL & Perez-Reyes E (1999). Nickel block of three cloned T-type calcium channels: low concentrations selectively block α_{1H}. *Biophys J* **77**, 3034–3042.

Lee S, Han TH, Ryu PD & Lee SY (2007). Molecular identification of ion channels for electrophysiological properties of rat hypothalamic neurons. *2007 Abstract Viewer/Itinerary Planner*, Programme No. 784.716. Society for Neuroscience, Washington, DC.

Lee S, Han TH, Sonner PM, Stern JE, Ryu PD & Lee SY (2008). Molecular characterization of T-type Ca^{2+} channels responsible for low threshold spikes in hypothalamic paraventricular nucleus neurons. *Neuroscience* **155**, 1195–1203.

Li DP & Pan HL (2006). Plasticity of GABAergic control of hypothalamic presympathetic neurons in hypertension. *Am J Physiol Heart Circ Physiol* **290**, H1110–1119.

Li M, Hansen JB, Huang L, Keyser BM & Taylor JT (2005). Towards selective antagonists of T-type calcium channels: design, characterization and potential applications of NNC 55-0396. *Cardiovasc Drug Rev* **23**, 173–196.

Li Y, Zhang W & Stern JE (2003). Nitric oxide inhibits the firing activity of hypothalamic paraventricular neurons that innervate the medulla oblongata: role of GABA. *Neuroscience* **118**, 585–601.

Li YF, Wang W, Mayhan WG & Patel KP (2006). Angiotensin-mediated increase in renal sympathetic nerve discharge within the PVN: role of nitric oxide. *Am J Physiol Regul Inegr Comp Physiol* **290**, R1035–1043.

Li Z & Ferguson AV (1996). Electrophysiological properties of paraventricular magnocellular neurons in rat brain slices: modulation of IA by angiotensin II. *Neuroscience* **71**, 133–145.

Livak KJ & Schmittgen TD (2001). Analysis of relative gene expression data using real-time quantitative PCR and the $2(-\Delta\Delta C_T)$ method. *Methods* **25**, 402–408.

Llinas R & Yarom Y (1981). Properties and distribution of ionic conductances generating electroresponsiveness of mammalian inferior olivary neurones *in vitro*. *J Physiol* **315**, 569–584.

Lovick TA & Coote JH (1988). Electrophysiological properties of paraventriculo-spinal neurones in the rat. *Brain Res* **454**, 123–130.

Luther JA & Tasker JG (2000). Voltage-gated currents distinguish parvocellular from magnocellular neurones in the rat hypothalamic paraventricular nucleus. *J Physiol* **523**, 193–209.

Mack SO, Kc P, Wu M, Coleman BR, Tolentino-Silva FP & Haxhiu MA (2002). Paraventricular oxytocin neurons are involved in neural modulation of breathing. *J Appl Physiol* **92**, 826–834.

Magee JC & Johnston D (2005). Plasticity of dendritic function. *Curr Opin Neurobiol* **15**, 334–342.

Martin DS & Haywood JR (1998). Reduced GABA inhibition of sympathetic function in renal-wrapped hypertensive rats. *Am J Physiol Regul Integr Comp Physiol* **275**, R1523–1529.

Martinez-Maldonado M (1991). Pathophysiology of renovascular hypertension. *Hypertension* **17**, 707–719.

McCobb DP & Beam KG (1991). Action potential waveform voltage-clamp commands reveal striking differences in calcium entry via low and high voltage-activated calcium channels. *Neuron* **7**, 119–127.

Meis S, Biella G & Pape HC (1996). Interaction between low voltage-activated currents in reticular thalamic neurons in a rat model of absence epilepsy. *Eur J Neurosci* **8**, 2090–2097.

Molineux ML, Fernandez FR, Mehaffey WH & Turner RW (2005). A-type and T-type currents interact to produce a novel spike latency-voltage relationship in cerebellar stellate cells. *J Neurosci* **25**, 10863–10873.

Monteil A, Chemin J, Bourinet E, Mennessier G, Lory P & Nargeot J (2000). Molecular and functional properties of the human α_{1G} subunit that forms T-type calcium channels. *J Biol Chem* **275**, 6090–6100.

Nagatomo T, Inenaga K & Yamashita H (1995). Transient outward current in adult rat supraoptic neurones with slice patch-clamp technique: inhibition by angiotensin II. *J Physiol* **485**, 87–96.

Narahashi T, Tsunoo A & Yoshii M (1987). Characterization of two types of calcium channels in mouse neuroblastoma cells. *J Physiol* **383**, 231–249.

Nesto RW (2004). Correlation between cardiovascular disease and diabetes mellitus: current concepts. *Am J Med* **116**(Suppl 5A), 11S–22S.

Nusser Z (2009). Variability in the subcellular distribution of ion channels increases neuronal diversity. *Trends Neurosci* **32**, 267–274.

Pape HC, Budde T, Mager R & Kisvarday ZF (1994). Prevention of Ca^{2+}-mediated action potentials in GABAergic local circuit neurones of rat thalamus by a transient K^+ current. *J Physiol* **478**, 403–422.

Parhar IS, Ogawa S, Hamada T & Sakuma Y (2003). Single-cell real-time quantitative polymerase chain reaction of immunofluorescently identified neurons of gonadotropin-releasing hormone subtypes in cichlid fish. *Endocrinology* **144**, 3297–3300.

Patel KP (2000). Role of paraventricular nucleus in mediating sympathetic outflow in heart failure. *Heart Fail Rev* **5**, 73–86.

Petty MA & Reid JL (1977). Changes in noradrenaline concentration in brain stem and hypothalamic nuclei during the development of renovascular hypertension. *Brain Res* **136**, 376–380.

Pinato G & Midtgaard J (2005). Dendritic sodium spikelets and low-threshold calcium spikes in turtle olfactory bulb granule cells. *J Neurophysiol* **93**, 1285–1294.

Raman IM & Bean BP (1999). Ionic currents underlying spontaneous action potentials in isolated cerebellar Purkinje neurons. *J Neurosci* **19**, 1663–1674.

Ranson RN, Motawei K, Pyner S & Coote JH (1998). The paraventricular nucleus of the hypothalamus sends efferents to the spinal cord of the rat that closely appose sympathetic preganglionic neurones projecting to the stellate ganglion. *Exp Brain Res* **120**, 164–172.

Rogawski MA (1985). The A-current: how ubiquitous a feature of excitable cells is it? *Trends Neurosci* **8**, 214–219.

Rudy B (1988). Diversity and ubiquity of K channels. *Neuroscience* **25**, 729–749.

Segal M, Rogawski MA & Barker JL (1984). A transient potassium conductance regulates the excitability of cultured hippocampal and spinal neurons. *J Neurosci* **4**, 604–609.
Sherman SM (2001). Tonic and burst firing: dual modes of thalamocortical relay. *Trends Neurosci* **24**, 122–126.
Sonner P & Stern JE (2006). Functional interactions between subthreshold A-type potassium (I_A) and T-type calcium currents (I_T) in RVLM-projecting PVN neurons in normotensive and hypertensive rats. *2006 Abstract Viewer/Itinerary Planner*, Programme No. 454.11. Society for Neuroscience, Washington, DC.
Sonner PM, Filosa JA & Stern JE (2007). Activity-dependent changes in intracellular Ca^{2+} dynamics in hypothalamic presympathetic PVN neurons. *2007 Abstract Viewer/Itinerary Planner*, Programme No. 85.88. Society for Neuroscience, Washington, DC.
Sonner PM, Filosa JA & Stern JE (2008). Diminished A-type potassium current and altered firing properties in presympathetic PVN neurones in renovascular hypertensive rats. *J Physiol* **586**, 1605–1622.
Sonner PM & Stern JE (2007). Functional role of A-type potassium currents in rat presympathetic PVN neurones. *J Physiol* **582**, 1219–1238.
Spanswick D & Renaud LP (2005). Angiotensin II induces calcium-dependent rhythmic activity in a subpopulation of rat hypothalamic median preoptic nucleus neurons. *J Neurophysiol* **93**, 1970–1976.
Stern JE (2001). Electrophysiological and morphological properties of pre-autonomic neurones in the rat hypothalamic paraventricular nucleus. *J Physiol* **537**, 161–177.
Stern JE & Armstrong WE (1995). Electrophysiological differences between oxytocin and vasopressin neurones recorded from female rats *in vitro*. *J Physiol* **488**, 701–708.
Stocker SD, Simmons JR, Stornetta RL, Toney GM & Guyenet PG (2006). Water deprivation activates a glutamatergic projection from the hypothalamic paraventricular nucleus to the rostral ventrolateral medulla. *J Comp Neurol* **494**, 673–685.
Swanson LW & Kuypers HG (1980). The paraventricular nucleus of the hypothalamus: cytoarchitectonic subdivisions and organization of projections to the pituitary, dorsal vagal complex, and spinal cord as demonstrated by retrograde fluorescence double-labeling methods. *J Comp Neurol* **194**, 555–570.
Swanson LW & Sawchenko PE (1983). Hypothalamic integration: organization of the paraventricular and supraoptic nuclei. *Annu Rev Neurosci* **6**, 269–324.
Tagawa T & Dampney RA (1999). AT_1 receptors mediate excitatory inputs to rostral ventrolateral medulla pressor neurons from hypothalamus. *Hypertension* **34**, 1301–1307.
Tasker JG & Dudek FE (1991). Electrophysiological properties of neurones in the region of the paraventricular nucleus in slices of rat hypothalamus. *J Physiol* **434**, 271–293.
Wang D, Sumners C, Posner P & Gelband CH (1997). A-type K^+ current in neurons cultured from neonatal rat hypothalamus and brain stem: modulation by angiotensin II. *J Neurophysiol* **78**, 1021–1029.
Wu ZZ, Li DP, Chen SR & Pan HL (2009). Aminopyridines potentiate synaptic and neuromuscular transmission by targeting the voltage-activated calcium channel β subunit. *J Biol Chem* **284**, 36453–36461.
Yang Z, Bertram D & Coote JH (2001). The role of glutamate and vasopressin in the excitation of RVL neurones by paraventricular neurones. *Brain Res* **908**, 99–103.
Yang Z & Coote JH (1998). Influence of the hypothalamic paraventricular nucleus on cardiovascular neurones in the rostral ventrolateral medulla of the rat. *J Physiol* **513**, 521–530.
Zheng H, Mayhan WG, Bidasee KR & Patel KP (2006). Blunted nitric oxide-mediated inhibition of sympathetic nerve activity within the paraventricular nucleus in diabetic rats. *Am J Physiol Regul Integr Comp Physiol* **290**, R992–R1002.
Zhu GQ, Gao L, Patel KP, Zucker IH & Wang W (2004). ANG II in the paraventricular nucleus potentiates the cardiac sympathetic afferent reflex in rats with heart failure. *J Appl Physiol* **97**, 1746–1754.

Author contributions

P.M.S.: collection, analysis and interpretation of electrophysiological, immunohistochemical and confocal imaging data; drafting of the article. S.L.: collection and analysis of PCR data. S.Y.L.: conception and design of PCR studies, interpretation of data, critical revision of the manuscript for intellectual content. P.D.R.: conception and design of PCR studies, interpretation of data, critical revision of the manuscript for intellectual content. J.E.S.: conception and design of electrophysiological and PCR studies; interpretation of data; drafting of the article. All authors approved the final version of the manuscript. This work was done at the Medical College of Georgia.

Acknowledgements

This work was supported by NIH R01 HL68725 (J.E.S.) and the National Research Foundation Grant 2010-0015531 (S.Y.L.).

Author's present address

P. M. Sonner: Department of Neuroscience, Cell Biology and Physiology, Wright State University, Dayton, OH, USA.